A EUROPEAN JOURNAL

CHEMPHYSCHEM

OF CHEMICAL PHYSICS AND PHYSICAL CHEMISTRY

Accepted Article

Title: Sub-ensemble monitoring of DNA strand displacement using multiparameter single-molecule FRET

Authors: Laura Baltierra-Jasso, Michael Morten, and Steven William Magennis

To be cited as: *ChemPhysChem* 10.1002/cphc.201800012

Link to VoR: http://dx.doi.org/10.1002/cphc.201800012

A Journal of

ChemPubSoc Europe

WILEY-VCH

www.chemphyschem.org

WILEY-VCH

COMMUNICATION

Sub-ensemble monitoring of DNA strand displacement using multiparameter single-molecule FRET

Laura E. Baltierra-Jasso, Michael J. Morten, and Steven W. Magennis*

Abstract: Non-enzymatic DNA strand displacement is an important mechanism in dynamic DNA nanotechnology. Here we show that the large parameter space that is accessible by single-molecule FRET is ideal for the simultaneous monitoring of multiple reactants and products of DNA strand exchange reactions. We monitored the strand displacement from double-stranded DNA (dsDNA) by single-stranded DNA (ssDNA) at 37 °C; the data were modelled as a second-order reaction approaching equilibrium, with a rate constant of ca. 10 M^{-1} s^{-1}. We also followed the displacement from a DNA three-way junction (3WJ) by ssDNA. The presence of three internal mismatched bases in the middle of the invading strand did not prevent displacement from the 3WJ, but reduced the second-order rate constant by ca. 50 %. We attribute strand exchange in the dsDNA and 3WJ to a zero-toehold pathway from the blunt-ended duplex arms. The single-molecule approach demonstrated here will be useful for studying complex DNA networks.

Nucleic acids can be employed as programmable nanostructural materials, taking advantage of Watson-Crick pairing.[1] By controlling the kinetics of base-pairing interactions, dynamic DNA nanosystems have been designed.[2] Dynamic control commonly utilizes toehold-mediated strand displacement, whereby a dsDNA with a short ssDNA overhang on one strand acts as the substrate for another ssDNA (the invader, which is complementary to the substrate); binding to the toehold and subsequent branch migration leads to strand displacement.[3] The kinetics of strand displacement in this three-way branch migration is dependent upon toehold length and is thought to be controlled by secondary structure at the branch migration junction and the relative rates of branch migration and base pair fraying.[4]

As the complexity of DNA networks increases, it will become increasingly important to monitor these heterogeneous and dynamic systems. A common method for studying DNA strand displacement is ensemble fluorescence spectroscopy.[5] In spite of the success and utility of bulk methods, single-molecule techniques offer distinct advantages, by avoiding the problems inherent in ensemble averaging.[6] For example, single-molecule Förster resonance energy transfer (smFRET) is well suited to the probing of nanoscale structure and dynamics.[7] There are now several examples of its application to DNA nanotechnology.[8-9]

In this work, we use smFRET to probe DNA strand displacement from either a blunt-ended double-stranded DNA (dsDNA) or a DNA three-way junction via invasion by a single-stranded DNA (ssDNA). We measure smFRET using multi-parameter fluorescence detection (MFD). MFD, pioneered by Seidel and co-workers, is a particularly powerful single-molecule fluorescence approach that is able to resolve multiple subpopulations in solution.[7b] By using pulsed laser excitation, and photon-counting detection and splitting the fluorescence according to polarization and color, all of the fluorescence properties are accessible at the single-molecule level. MFD has primarily been used in conjunction with FRET for probing biomolecular structure and dynamics.[10] Although less widely used, the extensive parameter space of MFD offers the possibility to resolve a large number of different sub-populations in a single sample. A notable demonstration of its analytical capabilities was the resolution of 16 different compounds in a solution mixture.[11] Here, we use MFD to follow strand exchange reactions via the unambiguous FRET signatures of the reactants and products as a function of time.

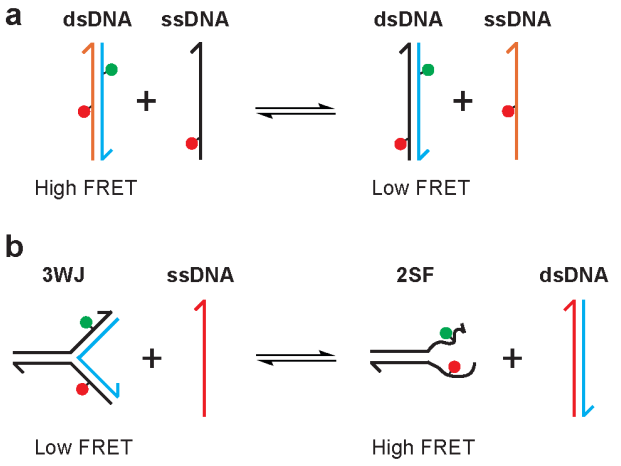

Scheme 1. FRET-based assay for monitoring strand displacement. a) For the dsDNA the forwards and backwards reactions are identical except for the positioning of the acceptor dyes. b) Displacement from the three-way junction (3WJ) produces a two-stranded fork (2SF) and dsDNA. The green and red circles represent the donor and acceptor dyes, respectively.

Our FRET-based approach is illustrated in Scheme 1. For the dsDNA, a pre-annealed 30bp duplex was labelled with a FRET donor (Alexa488) on one strand, and an acceptor dye (Cy5) on the other such that the dye-dye distance was short (12 base pairs), resulting in high FRET (Scheme 1a). This was mixed with a ssDNA that had an identical sequence to the Cy5-labeled strand in the duplex (black) but in which the Cy5 was in a different location. This ssDNA takes the role of the invader in the strand-displacement model. If strand displacement occurs, the duplex has the dyes farther apart, resulting in low FRET. The experiment involved incubating the pre-formed dsDNA (~0.6 μM) with a six-fold excess of the ssDNA strand (Tris buffer, pH 7.5, 10 mM

[a] Dr. L. E. Baltierra-Jasso,[+] Dr. M. J. Morten,[+] Dr. S. W. Magennis
WestCHEM School of Chemistry
University of Glasgow
University Avenue, Glasgow G128 QQ (UK)
E-mail: steven.magennis@glasgow.ac.uk

[+] These authors contributed equally to this work.

Supporting information for this article is given via a link at the end of the document.

$MgCl_2$) at 37 °C for up to 24 hours (see SI for DNA sequences and full details of sample preparation).

After incubation, the solution was diluted in buffer to the single-molecule level (*ca.* pM) and measured at 21 °C using MFD. Our MFD system uses a confocal microscope with pulsed laser excitation and four-channel photon-counting detection.[10d] The single-molecule FRET data (Figure 1) are plotted as 2D burst-frequency histograms of the ratio of the burst intensities in the green detection channels (S_G) for donor and red detection channels (S_R) for acceptor, S_G/S_R, or donor anisotropy (r_D) versus donor lifetime ($\tau_{D(A)}$). All plots contain a donor-only population with lifetime of ca. 4 ns, together with other populations of FRET-active molecules; FRET species have a decreased donor lifetime/intensity and increased acceptor intensity.

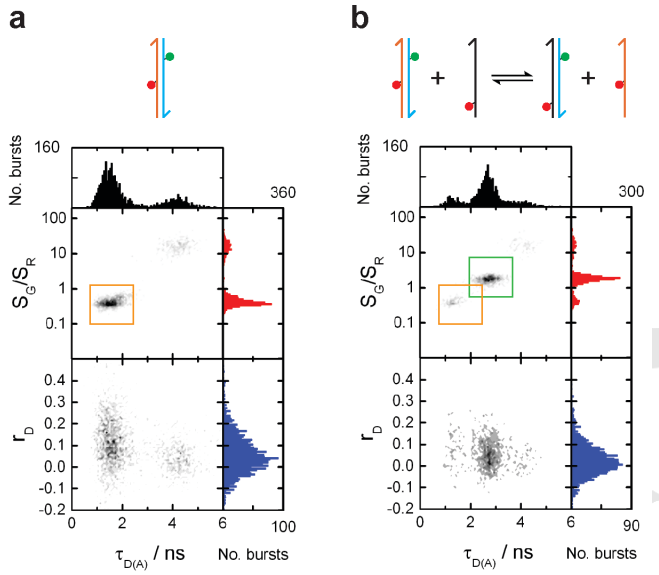

Figure 1. Single-molecule FRET at room temperature (21°C) after incubation for 24 h at 37 °C for (a) dsDNA (b) dsDNA + ssDNA invader strand. The dsDNA FRET populations are highlighted by the orange and green boxes. 2D burst-frequency histograms of the ratio of donor to acceptor signal (S_G/S_R) or donor anisotropy (r_D) versus donor lifetime ($\tau_{D(A)}$). All plots contain a donor-only population with lifetime of ca. 4 ns. The gray scale indicates an increasing number of single-molecule bursts (from white to black); also shown are the corresponding 1D histograms. See SI for sequences and experimental details.

In the absence of the invader strand the duplex population is clearly visible as the high-FRET population (Figure 1a). Incubation of the dsDNA at 37 °C caused strand displacement as shown by the appearance of a low-FRET population (Figure 1b). By measuring the numbers of molecules in each population, we calculated the fraction of displaced strands over a period of 24 hours (Figure 2). We model the kinetics of strand displacement as two second order reactions, which approach equilibrium exponentially (see SI for details). A plot of displacement vs time fitted well to such a model (Figure 2), giving a second-order rate constant of 10 ± 2 M^{-1} s^{-1} for the reaction of the dsDNA with the fully-complementary invader strand at 37 °C. From the fit, the equilibrium displacement is calculated as 85%, which is in excellent agreement with the ca. 86% displacement expected for the 1:6 ratio of the two acceptors strands. Therefore, the reaction had almost reached equlibrium after 24 hours, when the displacement was 83 ± 1 %.

We attribute the displacement to a blunt-end, zero-toehold mechanism. It is known that this occurs for dsDNA through reaction of unpaired bases[12] that are exposed at the end of a duplex due to DNA fraying.[13] Initial fraying from either the 3' or 5' end of the displaced strand acts as a site for invasion, followed by three-way branch migration. The rates we report are similar to those reported earlier for blunt-ended DNA duplexes.[4, 12a] Zero-toehold reactions are important as side reactions (or leakage), which can limit the programmability of complex dynamic DNA networks and circuits that utilize strand displacement.[14],[15] Our experiment involved reacting the dsDNA and invader strand at the micromolar level for 24h and then quenching the displacement reaction by diluting to picomolar concentrations at room temperature, followed by measurement at times up to several hours later; the cooling and dilution ensured that the reaction stopped. Since branch migration is believed to occur with a step time of ca. 10-100 μs,[4] we would not expect to observe any branch migration intermediates, in agreement with our single-molecule data.

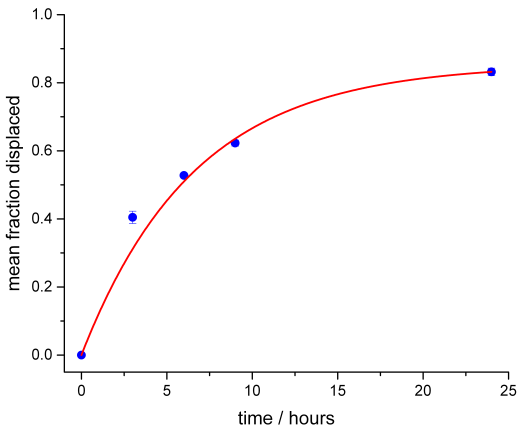

Figure 2. Displacement vs time for dsDNA at 37 °C. Data points and error bars in blue. The red line is a fit to a model of second-order reactions approaching equilibrium (see SI for details).

We also applied the same approach discussed for dsDNA to a branched DNA nanostructure, a 3WJ (Scheme 1b). Three- and four-way junctions are among the archetypal building blocks of DNA nanoscience,[16] and play important roles *in vivo*.[17] We recently used smFRET to probe the structure of a three-way junction (3WJ)[18] and found that there were unpaired bases at the branchpoint of a fully-complementary 3WJ, resulting in a nanoscale cavity.[18-19] This supported earlier accounts that 3WJs could bind supramolecular complexes at the branchpoint.[20] It also agreed with chemical footprinting experiments, which demonstrated that thymine bases at the 3WJ branchpoint were reactive to osmium tetroxide,[21] and to diethyl pyrocarbonate.[22]

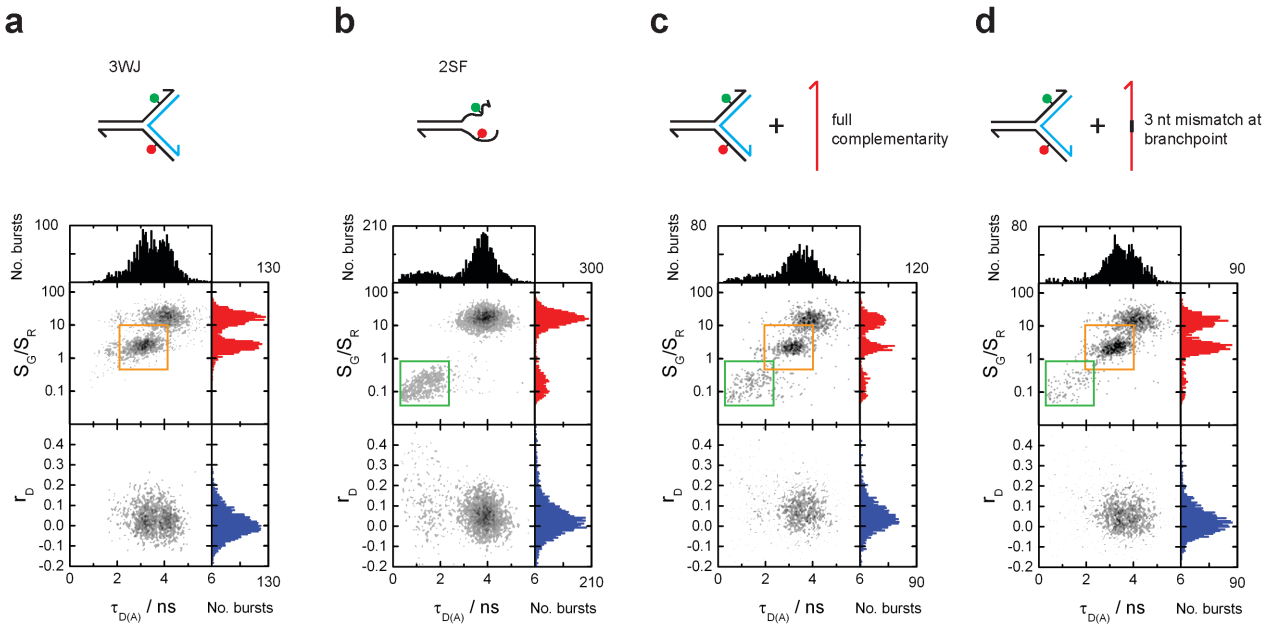

Figure 3. Single-molecule FRET at room temperature (21°C) after incubation for 24 h at 37 °C. a) 3WJ control b) 2SF control c) 3WJ + fully complementary invader strand and d) 3WJ + partially complementary invader strand. The 3WJ and 2SF FRET populations are highlighted by the orange and green boxes, respectively. See SI for sequences and experimental details. See Figure 1 legend for details of the MFD plots, and the SI for sequences and experimental details.

Two strands of an immobile 3WJ were labeled with either a donor (Alexa488) or acceptor dye (Cy5). This was mixed with a ssDNA (red) that was complementary to the unlabeled strand of the 3WJ (blue). The products of strand displacement would be unlabeled dsDNA and a two-stranded forked DNA molecule (2SF). The 3WJ studied here has been reported previously by us,[19] and consists of three 50mer strands designed to form a fully-complementary 3WJ after annealing (see Figure S1). The experiment involved incubating the pre-formed 3WJ (~0.6 μM) with a six-fold excess of a 50mer ssDNA strand (Tris buffer, pH 7.5, 10 mM $MgCl_2$) at 37 °C for up to 24 hours. Two 50mer strands were studied: one strand had full complementarity with one of the 3WJ strands, while a second 50mer was mismatched with the 3WJ strand at three bases at the branchpoint.

MFD data for the 3WJ and the target product (the 2SF) are shown in Figures 3a and 3b, respectively. The dyes are attached to ssDNA in the 2SF, which means that they are in closer proximity than in the 3WJ, resulting in a large increase in FRET. After incubating the mixture of the 3WJ with the fully-complementary ssDNA at 37 °C for 24h (Figure 3c) we observed two FRET populations that matched exactly those of the control samples of 3WJ and 2SF. The fraction of displaced strands after 24 hours was 26 ± 5 %. After repeating this experiment using the mismatched strand, we observed the same two FRET populations (Figure 3d), but this time the fraction displaced after 24 hours was reduced to 13 ± 2 %. The fraction of displaced molecules as a function of time is shown in Figure S2. Unlike the dsDNA reaction, the forward and backwards reactions are no longer equivalent. We heated reaction mixtures to 90°C and measured after cooling to 21 °C. For the fully-complementary ssDNA, all of the 3WJ was converted to 2SF; for the partially-complementary ssDNA, only a small 3WJ population remained (Figure S3). This shows that reaction is far from equilibrium after 24 hours at 37 °C.

We used NUPACK[23] to estimate the free energies of reactants and products (see Figures S4-8 and Table S1). The calculations suggest that the products (dsDNA and 2SF) are strongly thermodynamically favoured when the ssDNA is fully-complementary but slightly disfavoured when the partially-complementary ssDNA is used. This is in broad agreement with our MFD data, given the simplification of our kinetic scheme. NUPACK also predicts that secondary structures can form for 2SF (Fig. S6). This agrees with the very broad 2SF population (c.f. the narrow high-FRET distribution for dsDNA in Fig. 1a), which is indicative of structural heterogeneity.

Based on the MFD data and NUPACK calculations, the reaction of 3WJ and ssDNA at 37 °C is likely to be more complex than that of dsDNA and ssDNA. However, we found that it could be reasonably approximated as an irreversible second-order reaction (Figure 4). The rate constant for the reaction of the fully-complementary ssDNA and 3WJ was 1 ± 0.1 M^{-1} s^{-1}, which is an order of magnitude smaller than that calculated for the dsDNA. The rate constant for the mismatched ssDNA and 3WJ was reduced by half (0.5 ± 0.1 M^{-1} s^{-1}) compared with the fully-complementary ssDNA. We had speculated that the bases at the branchpoint of the 3WJ might be accessible as an internal toehold by a complementary DNA strand in a sequence-dependent manner, leading to branch migration and strand displacement. However, since toehold-mediated strand displacement can be faster by a factor of up to 10^6,[4-5] and since this rate should be very sensitive to losing three bases of the toehold (i.e. in the

mismatched ssDNA) we believe that a zero-toehold mechanism predominates.

Nevertheless, three mismatched bases in the ssDNA might be expected to impede the branch migration process. It is known that mismatches in the toehold region can have a large effect on the rate of strand displacement[24] and even a single mismatched internal base can be enough to significantly slow branch migration.[24b] However, this effect was shown to weaken the further the mismatch was from the toehold, being negligible after 14 bases.[24b] It has also been reported that up to 4 contiguous internal mismatches were required to significantly slow three-way branch migration in dsDNA.[25] The mismatched bases in the 3WJ studied here are 24 or 25 bases away from the blunt-end of the duplex where the reaction initiates. Since we believe that the bases at the 3WJ branchpoint are, at least transiently, unpaired,[18-19] mismatches at the branchpoint should be even less of a barrier.

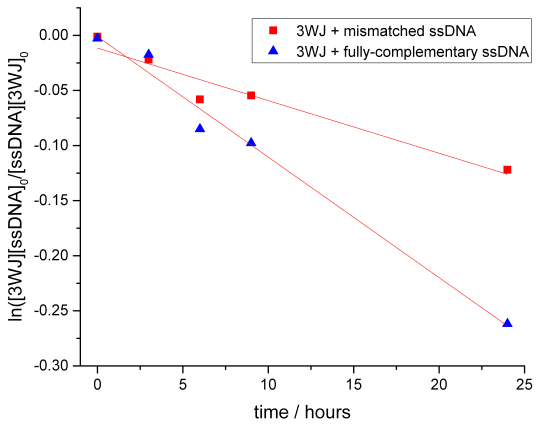

Figure 4. Displacement vs time for 3WJ at 37 °C. The fits are for a second-order reaction: 3WJ + ssDNA → 2SF + dsDNA (see SI for details).

Assuming each branch migration step takes the same average time, then we would expect the rate to scale with 1/N, where N is the number of base pairs (30 for the dsDNA and 50 for the 3WJ).[4] This alone does not account for the order of magnitude difference in second-order rate constants for the reaction of dsDNA and 3WJ. As discussed, zero-toehold exchange involves fraying of base pairs at the blunt end. Even a single toehold can account for ca. an order of magnitude increase in rate.[26] NUPACK estimated the probability of opening of the end basepairs in question for the 3WJ as 0.77 (GC) and 0.48 (AT), while for the dsDNA these were 0.51 (AT) and 0.22 (AT). One AT basepair in each structure has a similar opening probability while the other basepair in the 3WJ is 3.5 times more likely to be closed than in the dsDNA. The increased availability of the toehold on dsDNA, along with its shorter length can account for the difference in rate constants.

This work demonstrates the ability of multi-parameter smFRET to probe the reaction pathways and rates of dynamic DNA systems. We studied zero-toehold displacement, an important leakage pathway. Monitoring multiple species simultaneously is a powerful approach and we anticipate that this will be used in future to probe more complex DNA networks, taking full advantage of the large parameter space available.

Acknowledgements

We thank the EPSRC for support of MJM (EP/L027003/1); LEBJ thanks CONACyT for the award of a scholarship.

Keywords: DNA • nanostructures • nanotechnology • multiparameter • fluorescence

[1] M. R. Jones, N. C. Seeman, C. A. Mirkin, *Science* **2015**, *347*, 840-+.
[2] a) B. Yurke, A. J. Turberfield, A. P. Mills, F. C. Simmel, J. L. Neumann, *Nature* **2000**, *406*, 605-608; b) D. Y. Zhang, G. Seelig, *Nature Chem.* **2011**, *3*, 103-113; c) F. Wang, C.-H. Lu, I. Willner, *Chem. Rev.* **2014**, *114*, 2881-2941; d) H. Z. Gu, J. Chao, S. J. Xiao, N. C. Seeman, *Nature* **2010**, *465*, 202-205; e) K. Lund, A. J. Manzo, N. Dabby, N. Michelotti, A. Johnson-Buck, J. Nangreave, S. Taylor, R. J. Pei, M. N. Stojanovic, N. G. Walter, E. Winfree, H. Yan, *Nature* **2010**, *465*, 206-210.
[3] a) C. M. Radding, K. L. Beattie, W. K. Holloman, R. C. Wiegand, *J. Mol. Biol.* **1977**, *116*, 825-839; b) C. Green, C. Tibbetts, *Nucleic Acids Res.* **1981**, *9*, 1905-1918; c) I. G. Panyutin, P. Hsieh, *Proc. Natl. Acad. Sci. USA* **1994**, *91*, 2021-2025.
[4] N. Srinivas, T. E. Ouldridge, P. Sulc, J. M. Schaeffer, B. Yurke, A. A. Louis, J. P. K. Doye, E. Winfree, *Nucleic Acids Res.* **2013**, *41*, 10641-10658.
[5] D. Y. Zhang, E. Winfree, *J. Am. Chem. Soc.* **2009**, *131*, 17303-17314.
[6] W. E. Moerner, *Angew. Chem. Int. Ed.* **2015**, *54*, 8067-8093.
[7] a) R. Roy, S. Hohng, T. Ha, *Nat. Methods* **2008**, *5*, 507-516; b) E. Sisamakis, A. Valeri, S. Kalinin, P. J. Rothwell, C. A. M. Seidel, *Methods Enzymol.* **2010**, *475*, 455-514.
[8] B. K. Mueller, A. Reuter, F. C. Simmel, D. C. Lamb, *Nano Lett.* **2006**, *6*, 2814-2820.
[9] R. Tsukanov, T. E. Tomov, M. Liber, Y. Berger, E. Nir, *Acc. Chem. Res.* **2014**, *47*, 1789-1798.
[10] a) S. Kalinin, T. Peulen, S. Sindbert, P. J. Rothwell, S. Berger, T. Restle, R. S. Goody, H. Gohlke, C. A. M. Seidel, *Nat. Methods* **2012**, *9*, 1218-U1129; b) A. K. Woźniak, G. F. Schröder, H. Grubmüller, C. A. M. Seidel, F. Oesterhelt, *Proc. Natl. Acad. Sci. USA* **2008**, *105*, 18337-18342; c) V. Kudryavtsev, M. Sikor, S. Kalinin, D. Mokranjac, C. A. M. Seidel, D. C. Lamb, *Chemphyschem* **2012**, *13*, 1060-1078; d) T. Sabir, G. F. Schröder, A. Toulmin, P. McGlynn, S. W. Magennis, *J. Am. Chem. Soc.* **2011**, *133*, 1188-1191.
[11] J. Widengren, V. Kudryavtsev, M. Antonik, S. Berger, M. Gerken, C. A. M. Seidel, *Anal. Chem.* **2006**, *78*, 2039-2050.
[12] a) L. P. Reynaldo, A. V. Vologodskii, B. P. Neri, V. I. Lyamichev, *J. Mol. Biol.* **2000**, *297*, 511-520; b) A. A. Neschastnova, V. K. Markina, V. I. Popenko, O. A. Danilova, R. A. Sidorov, G. A. Belitsky, M. G. Yakubovskaya, *Biochemistry* **2002**, *41*, 7795-7801.
[13] a) D. Jose, K. Datta, N. P. Johnson, P. H. von Hippel, *Proc. Natl. Acad. Sci. USA* **2009**, *106*, 4231-4236; b) D. Andreatta, S. Sen, J. L. P. Lustres, S. A. Kovalenko, N. P. Ernsting, C. J. Murphy, R. S. Coleman, M. A. Berg, *J. Am. Chem. Soc.* **2006**, *128*, 6885-6892.
[14] X. Olson, S. Kotani, J. E. Padilla, N. Hallstrom, S. Goltry, J. Lee, B. Yurke, W. L. Hughes, E. Graugnard, *ACS Synth. Biol.* **2017**, *6*, 84-93.
[15] S. Kotani, W. L. Hughes, *J. Am. Chem. Soc.* **2017**, *139*, 6363-6368.
[16] N. C. Seeman, N. R. Kallenbach, *Annu. Rev. Biophys. Biomol. Struct.* **1994**, *23*, 53-86.
[17] D. M. J. Lilley, *Q. Rev. Biophys.* **2000**, *33*, 109-159.
[18] T. Sabir, A. Toulmin, L. Ma, A. C. Jones, P. McGlynn, G. F. Schroeder, S. W. Magennis, *J. Am. Chem. Soc.* **2012**, *134*, 6280-6285.
[19] A. Toulmin, L. E. Baltierra-Jasso, M. J. Morten, T. Sabir, P. McGlynn, G. F. Schröder, B. O. Smith, S. W. Magennis, *Biochemistry* **2017**, *56*, 4985–4991.
[20] A. Oleksi, A. G. Blanco, R. Boer, I. Usón, J. Aymamí, A. Rodger, M. J. Hannon, M. Coll, *Angew. Chem. Int. Ed.* **2006**, *45*, 1227-1231.
[21] D. R. Duckett, D. M. J. Lilley, *EMBO J.* **1990**, *9*, 1659-1664.
[22] G. Qiu, L. Min, M. E. A. Churchill, T. D. Tullius, N. R. Kallenbach, *Biochemistry* **1990**, *29*, 10927-10934.
[23] J. N. Zadeh, C. D. Steenberg, J. S. Bois, B. R. Wolfe, M. B. Pierce, A. R. Khan, R. M. Dirks, N. A. Pierce, *J. Comput. Chem.* **2011**, *32*, 170-173.
[24] a) Y. S. Jiang, S. Bhadra, B. Li, A. D. Ellington, *Angew. Chem. Int. Ed.* **2014**, *53*, 1845-1848; b) R. R. F. Machinek, T. E. Ouldridge, N. E. C. Haley, J. Bath, A. J. Turberfield, *Nat. Commun.* **2014**, *5*; c) D. W. B. Broadwater, H. D. Kim, *Biophys. J.* **2016**, *110*, 1476-1484.
[25] I. G. Panyutin, P. Hsieh, *J. Mol. Biol.* **1993**, *230*, 413-424.
[26] B. Yurke, A. P. Mills, *Genet. Program. Evolvable Mach.* **2003**, *4*, 111-122.

10.1002/cphc.201800012

WILEY-VCH

Entry for the Table of Contents

COMMUNICATION

*Author(s), Corresponding Author(s)**

Page No. – Page No.

Title

The reaction of DNA nanostructures is monitored using single-molecule FRET